Biochemical and Biophysical Research Communications 431 (2013) 437–443

Contents lists available at SciVerse ScienceDirect

Biochemical and Biophysical Research Communications

journal homepage: www.elsevier.com/locate/ybbrc

# Differential expression analysis throughout the weaning period in the mouse cerebral cortex

Naohiro Maeda [a,2], Shinpei Kawakami [a,2], Makoto Ohmoto [a,1], Johannes le Coutre [b,c], Gerard Vinyes-Pares [c,d], Fabrizio Arigoni [c,d], Shinji Okada [a], Keiko Abe [a], Hiroyuki Aizawa [a,*], Takumi Misaka [a,*]

[a] Department of Applied Biological Chemistry, Graduate School of Agricultural and Life Sciences, The University of Tokyo, 1-1-1 Yayoi, Bunkyo-ku, Tokyo 113-8657, Japan
[b] Perception Physiology, Nestlé Research Center, Vers-chez-les-Blanc, Lausanne, Switzerland
[c] Organization for Interdisciplinary Research Projects, The University of Tokyo, Tokyo, Japan
[d] Nestlé Research Tokyo, Nestlé Ltd., 1-1-1 Yayoi, Bunkyo-ku, Tokyo, Japan

ARTICLE INFO

*Article history:*
Received 12 December 2012
Available online 16 January 2013

*Keywords:*
Taste signal
Weaning period
Gustatory cortex
Somatosensory cortex
Immediate early gene

ABSTRACT

At weaning, mammals switch from drinking mother's milk to eating foods of environmental origin. These foods contain natural compounds with novel tastes and textures, which are provided to the young for the first time following the termination of breastfeeding. This novel eating experience may alter the cognitive brain function of mammalian babies, increasing their reactions to their food environments. Because the cerebral cortex is a central organ for cognition and learning, we investigated differences in whole-gene expression profiles in the mouse cerebral cortex using microarray analysis before and after weaning. Of 45,037 murine genes, 35 genes were upregulated and 31 genes were downregulated, in response to weaning. In particular, immediate early genes, molecular chaperones, and myelin-related genes were upregulated. *In situ* hybridization analysis revealed that the mRNA for an immediate early gene, Egr-2/KROX-20, was transported from the nucleus to the cell body at layer 5/6 of the somatosensory cortex during weaning. In contrast, in animals without any food supply other than mother's milk, Egr-2/KROX-20 mRNA was retained within the nucleus at the somatosensory cortex. These data suggest that the novel experience of food intake modulates gene expression profiles in the murine cerebral cortex at the weaning stage.



## 1. Introduction

It is well known that dietary food experience, especially at a younger stage, evokes personal food preferences, which are generally maintained throughout the life [1]. Food not only supplies energy and building blocks to our body but also has chemo-functional effects, which are detected through taste and smell via its chemical and physical properties [2–6]. In the development of the visual system, it is well established that optical experience plays a central role in determining the projection pattern of the thalamocortical optic nerve onto the cerebral visual cortex. This is particularly true at a childhood stage called the "critical period" [7]. In the development of the gustatory system, little is known about this type of neuronal plasticity for the cognitive processing of food signals.

Shortly after birth, mammals begin to drink their mother's breast milk, which is a complete and nutritious food adapted for the optimal growth of babies during infancy. As the lactation period progresses, mammals begin to eat various types of weaning foods, whose taste, texture, and nutrition are quite variable depending on their natural environments. It is critical for health research to understand how these natural foods affect mammalian taste and cognitive development in childhood and later in life [8].

Taste and somatosensory signals, including sweet, salty, bitter, umami, sour, texture, hot, cool, and spicy, are recognized in the oral cavity and in the intestine [2–6]. These sensory organs are innervated by peripheral gustatory and somatosensory neurons from the peripheral ganglia [9–11]. Afferent taste and somatosensory signals are eventually projected onto the gustatory and somatosensory cortex, respectively, within the central nervous system [12–20].

Experience-dependent neuronal plasticity may be established by novel gene expression, pre-existing protein modification, and cell survival and death induced by neuronal stimulation of the sensory system [21]. To understand the molecular mechanism of developmental neural plasticity of the taste sensory and cognitive systems, we investigated a genome-wide expression profile of the

* Corresponding authors. Fax: +81 3 5841 8100.
*E-mail addresses:* aaizawa@mail.ecc-u-tokyo.ac.jp (H. Aizawa), amisaka@mail.ecc.u-tokyo.ac.jp (T. Misaka).
[1] Present address: Monell Chemical Senses Center, Philadelphia, PA 19104-3308, United States.
[2] These authors contributed equally to this work.

0006-291X/$ - see front matter © 2013 Elsevier Inc. All rights reserved.
http://dx.doi.org/10.1016/j.bbrc.2012.12.150

murine gustatory cortex using microarray analysis. We found that a subset of genes was upregulated or downregulated by food intake experience during weaning.

## 2. Materials and methods

### 2.1. Animals

All procedures performed in this study were approved by the Animal Care and Use Committee of the University of Tokyo and were performed in accordance with the National Institutes of Health's Guide for the Care and Use of Laboratory Animals. All efforts were made to minimize the number of animals used and the duration of their suffering. All procedures for animal maintenance and experiments were performed as described previously [20]. Briefly, all mice were purchased on postnatal day 7 with their mother from CLEA Japan (Tokyo, Japan) and maintained with free access to CLEA Rodent diet OA-2 (CLEA Japan) and bottled water until experiments were initiated. Stimulation of weaning mice with or without solid food intake was performed as previously described [20]. Briefly, two cages were prepared, one of which was supplied with solid meal CLEA Rodent diet OA-2 (CLEA Japan) while the other was not. Each cage contained one mother and six pups, and the two mothers were exchanged every 12 h for feeding. Thus, mother mice were partly restricted from food access during this experiment.

### 2.2. Microarray analysis of the gustatory and somatosensory cortices

For each microarray analysis, three male mice were euthanized and the whole brain was dissected out using standard procedures. The brain was put onto the dissection apparatus, pre-cooled on ice, and sliced using razor blades at 2-mm thicknesses. Then, under microscopic observation, the gustatory and somatosensory cortices were dissected out using forceps. Right and left cortices from a single animal were collected and combined for a single analysis. RNA preparation was performed using TRIzol reagent (Invitrogen) as described previously [22]. For microarray analysis, amplified cRNA was prepared using the 3′IVT Express Kit (Affymetrix) and the GeneChip Mouse Genome 430A 2.0 Array (Affymetrix) as previously described [22]. Microarray analysis was performed as described previously [22]. Briefly, we prepared three individual RNA samples for each microarray analysis experiment on p15, p20, p23, and p28. Genes displaying a signal intensity of more than 200 on at least 1 day among p15, p20, p23, and p30 were analyzed. Then, we selected genes with a corresponding signal on one of the 4 days that was more than twice as intense as the signal on one of the three other days. Finally, we confirmed the significance of changes in the expression level of the genes by false discovery rate (FDR) analysis (Tukey's test) with less than 0.20 between at least one set of the four experiments.

### 2.3. In situ hybridization

*In situ* hybridization was performed as previously described [11]. Complementary DNA of Egr-2/KROX20 was a generous gift from Dr. Jeffrey D. Milbrandt (Washington University, MO). Complementary RNA probes were prepared using T3/T7 RNA polymerase as previously described [11]. Briefly, cerebral coronal specimens were observed and photographed using an Olympus Inverted Microscope (Olympus, Japan). Both gustatory and somatosensory cortices (bregma +0.85 mm) were studied, especially at layer 5 on postnatal days 15 and 22. To quantify punctate mRNA, we processed the digital image using Adobe Photoshop, and we counted the number of RNA punctate signals with greater intensity

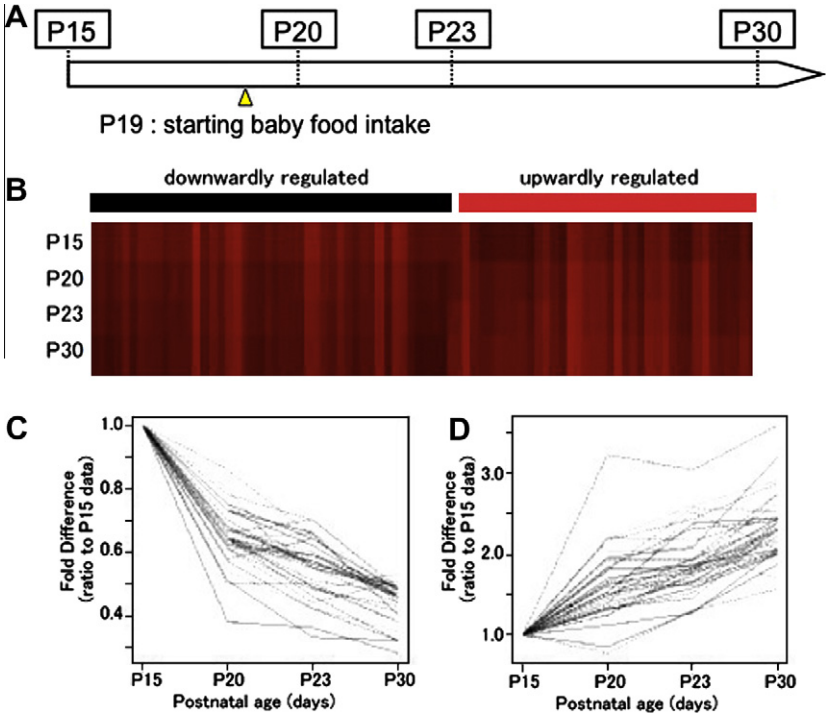


**Fig. 1.** Microarray analysis of the gustatory and somatosensory cortex during the weaning period. (A) Experimental schedule and murine weaning period during development. P15: postnatal day 15; P20: postnatal day 23; P23: postnatal day 23; P30: postnatal day 30. (B) Heat map of upregulated (right) and downregulated (left) genes showing the mean expression level by red color intensity. (C) Time course of the expression level of the downregulated genes. The mean expression level on postnatal day 15 was set to 1 for each gene expression profile. Thirty-one genes in Table 1A were plotted. (D) Time course of the expression level of the upregulated genes. The mean expression level on postnatal day 15 was set to 1 for each gene expression profile. Thirty-five genes in Table 1B were plotted.

**Table 1**
Genes upregulated and downregulated in the gustatory and somatosensory cortices during the weaning period. Gene function is cited from Net Affix. All of the changed primer sets are represented by their gene symbols. Thirty-one genes represented by 45 primer sets were downregulated (A), and 35 genes represented by 39 primer sets were upregulated (B).

| Gene symbol | Gene title | | | | | Change (fold) | | | FDR (Tukey) | | |
|---|---|---|---|---|---|---|---|---|---|---|---|
| | | GC (P15) | GC (P20) | GC (P23) | GC (P30) | P20/P15 | P23/P15 | P30/P15 | P15 vs P20 | P15 vs P23 | P15 vs P30 |
| *A. Upwardely regulated genes* | | | | | | | | | | | |
| Malat1 | Metastasis-associated lung adenocarcinoma transcript 1 (non-coding RNA) | 230.3 | 194.9 | 298.1 | 433.9 | 0.846 | 1.29 | 1.88 | 1 | 0.849 | 0.148 |
| Nedd4 | Neural precursor cell expressed, developmentally down-regulated 4 | 293.9 | 226.2 | 381.1 | 460.5 | 0.77 | 1.3 | 1.57 | 0.824 | 0.807 | 0.339 |
| Malat1 | Metastasis-associated lung adenocarcinoma transcript 1 (non-coding RNA) | 1092.8 | 1071.9 | 1902.2 | 2229.8 | 0.981 | 1.74 | 2.04 | 1 | 0.162 | 0.057 |
| Mog | Myelin oligodendrocyte glycoprotein | 172.3 | 349.7 | 356.6 | 291.2 | 2.03 | 2.07 | 1.69 | 0.146 | 0.125 | 0.315 |
| Cbln4 | Cerebellin 4 precursor protein | 87.2 | 166.5 | 167.4 | 229.2 | 1.91 | 1.92 | 2.63 | 0.114 | 0.105 | 0.017 |
| Egr2 | Early growth response 2 | 97.9 | 191.2 | 189.9 | 269.6 | 1.95 | 1.94 | 2.75 | 0.5 | 0.486 | 0.156 |
| Dnajc21 | DnaJ (Hsp40) homolog, subfamily C, member 21 | 141.7 | 277.6 | 294.1 | 453.8 | 1.96 | 2.08 | 3.2 | 0.002 | 0.001 | 0 |
| Phf15 | PHD finger protein 15 | 136.5 | 296.5 | 332 | 392.8 | 2.17 | 2.43 | 2.88 | 0 | 0 | 0 |
| Ermn | Ermin, ERM-like protein | 128 | 280.5 | 332.6 | 372.9 | 2.19 | 2.6 | 2.91 | 0.09 | 0.036 | 0.019 |
| Hspa1b | Heat shock protein 1B | 145.3 | 261.8 | 372.7 | 368.2 | 1.8 | 2.57 | 2.53 | 0 | 0 | 0 |
| Hapln4 | Hyaluronan and proteoglycan link protein 4 | 94.5 | 140.5 | 183.7 | 225.2 | 1.49 | 1.94 | 2.38 | 0.379 | 0.069 | 0.019 |
| Arc | Activity-regulated cytoskeletal-associated protein | 259.3 | 397.3 | 617.3 | 635.2 | 1.53 | 2.38 | 2.45 | 0.192 | 0.008 | 0.006 |
| Erdr1 | Erythroid differentiation regulator 1 | 565.8 | 779.2 | 1431 | 1158 | 1.38 | 2.53 | 2.05 | 0.825 | 0.065 | 0.161 |
| Igfbp6 | Insulin-like growth factor binding protein 6 | 194.5 | 324.4 | 376 | 422.1 | 1.67 | 1.93 | 2.17 | 0.137 | 0.048 | 0.021 |
| Emb | Embigin | 111 | 159.5 | 197.8 | 222.6 | 1.44 | 1.78 | 2.01 | 0.001 | 0 | 0 |
| C330006P03Rik | GLGF-domain protein Homer | 1372.7 | 2522.6 | 3188.6 | 3307.6 | 1.84 | 2.32 | 2.41 | 0.002 | 0 | 0 |
| Mobp | Myelin-associated oligodendrocytic basic protein | 1219.2 | 2073.4 | 2283 | 2517.1 | 1.7 | 1.87 | 2.06 | 0.194 | 0.104 | 0.052 |
| Mobp | Myelin-associated oligodendrocytic basic protein | 505.9 | 840 | 877.1 | 1139.8 | 1.66 | 1.73 | 2.25 | 0.347 | 0.269 | 0.066 |
| Bhlhe40 | Basic helix–loop–helix family, member e40 | 497.8 | 758.3 | 819.2 | 999.5 | 1.52 | 1.65 | 2.01 | 0.037 | 0.016 | 0.002 |
| Pvalb | Parvalbumin | 439.6 | 787 | 797 | 892.4 | 1.79 | 1.81 | 2.03 | 0.361 | 0.33 | 0.189 |
| Gstm1 | glutathione S-transferase, mu 1 | 189.8 | 304.6 | 305 | 390.9 | 1.6 | 1.61 | 2.06 | 0.037 | 0.034 | 0.003 |
| Pdp1 | Pyruvate dehyrogenase phosphatase catalytic subunit 1 | 979.1 | 1590 | 1783.3 | 2258.5 | 1.62 | 1.82 | 2.31 | 0.004 | 0.001 | 0 |
| Rims3 | Regulating synaptic membrane exocytosis 3 | 183.1 | 240.7 | 288.8 | 367 | 1.31 | 1.58 | 2 | 0.137 | 0.014 | 0.001 |
| Trf | Transferrin | 318.4 | 470.2 | 576.7 | 746.9 | 1.47 | 1.81 | 2.35 | 0.296 | 0.068 | 0.011 |
| Ier3 | Immediate early response 3 | 122.1 | 170.5 | 202.4 | 270 | 1.4 | 1.66 | 2.21 | 0.012 | 0.001 | 0 |
| Malat1 | Metastasis associated lung adenocarcinoma transcript 1 (non-coding RNA) | 597.1 | 725.9 | 1105 | 1470.9 | 1.22 | 1.85 | 2.46 | 0.918 | 0.087 | 0.014 |
| Atp2b2 | ATPase, Ca++ transporting, plasma membrane 2 | 489.7 | 610.3 | 907.2 | 1047.3 | 1.25 | 1.85 | 2.14 | 0.869 | 0.097 | 0.037 |
| Plekhb1 | Pleckstrin homology domain containing, family B (evectins) member 1 | 769.5 | 1031.4 | 1331.7 | 1770.1 | 1.34 | 1.73 | 2.3 | 0.205 | 0.014 | 0.001 |
| 3021401C12Rik | RIKEN cDNA 3021401C12 gene | 182.7 | 332.6 | 337.2 | 445 | 1.82 | 1.85 | 2.44 | 0.001 | 0.001 | 0 |
| Plekhh1 | Pleckstrin homology domain containing, family H (with MyTH4 domain) member 1 | 116.9 | 193.2 | 206.8 | 270.1 | 1.65 | 1.77 | 2.31 | 0.045 | 0.023 | 0.003 |
| Ier5 | Immediate early response 5 | 96.2 | 156.9 | 160.3 | 219.4 | 1.63 | 1.67 | 2.28 | 0.056 | 0.043 | 0.003 |
| Mal | Myelin and lymphocyte protein, T-cell differentiation protein | 402.5 | 885.2 | 867.8 | 992.3 | 2.2 | 2.16 | 2.47 | 0.053 | 0.056 | 0.024 |
| Mal | Myelin and lymphocyte protein, T-cell differentiation protein | 784.5 | 1915.6 | 1894.8 | 2379 | 2.44 | 2.42 | 3.03 | 0.059 | 0.06 | 0.019 |
| 2900052N01Rik | RIKEN cDNA 2900052N01 gene | 240.7 | 320.8 | 349.2 | 557.6 | 1.33 | 1.45 | 2.32 | 0.29 | 0.125 | 0.002 |
| Il33 | Interleukin 33 | 152.1 | 170.8 | 192.7 | 311 | 1.12 | 1.27 | 2.04 | 0.616 | 0.091 | 0 |
| Dnajc21 | DnaJ (Hsp40) homolog, subfamily C, member 21 | 156.5 | 204.9 | 238.3 | 377.8 | 1.31 | 1.52 | 2.41 | 0.527 | 0.161 | 0.005 |
| C920025E04Rik | RIKEN cDNA C920025E04 gene///histocompatibility 2, T region locus 23 | 138.6 | 193.4 | 228.1 | 310.4 | 1.4 | 1.65 | 2.24 | 0.069 | 0.01 | 0.001 |
| Igh-6 | Immunoglobulin heavy chain 6 (heavy chain of IgM) | 269.9 | 333.9 | 477.7 | 742 | 1.24 | 1.77 | 2.75 | 0.933 | 0.177 | 0.015 |
| Scn4b | Sodium channel, type IV, beta | 80.1 | 258.7 | 243 | 288.3 | 3.23 | 3.03 | 3.6 | 0.019 | 0.023 | 0.01 |
| *B. Downwardly regulated genes* | | | | | | | | | | | |
| Gm9106 | Predicted gene 9106///MARCKS-like 1 | 209.3 | 153.4 | 138.1 | 84.5 | 0.733 | 0.66 | 0.404 | 0 | 0 | 0 |
| Sla | src-like adaptor | 285.9 | 245.9 | 186.8 | 125.6 | 0.86 | 0.653 | 0.439 | 0.912 | 0.127 | 0.005 |
| Marcksl1 | MARCKS-like 1 | 215.4 | 148.2 | 124.4 | 76.6 | 0.688 | 0.578 | 0.356 | 0.011 | 0.001 | 0 |
| Tet1 | tet oncogene 1 | 334.9 | 237.3 | 156.2 | 125.3 | 0.709 | 0.466 | 0.374 | 0.007 | 0 | 0 |
| Dpysl3 | Dihydropyrimidinase-like 3 | 858 | 462.6 | 364.2 | 304.5 | 0.539 | 0.424 | 0.355 | 0.091 | 0.02 | 0.007 |
| Ctla2a | Cytotoxic T lymphocyte-associated protein 2 alpha | 277.3 | 181.5 | 136.9 | 114.1 | 0.655 | 0.494 | 0.411 | 0.003 | 0 | 0 |
| Cd24a | CD24a antigen | 694.9 | 394.1 | 294.4 | 220.8 | 0.567 | 0.424 | 0.318 | 0.004 | 0 | 0 |
| Dpysl3 | Dihydropyrimidinase-like 3 | 586.6 | 307.3 | 227.8 | 192.8 | 0.524 | 0.388 | 0.329 | 0.112 | 0.02 | 0.008 |
| Cxadr | Coxsackie virus and adenovirus receptor | 545.1 | 277.4 | 177.6 | 172.4 | 0.509 | 0.326 | 0.316 | 0.006 | 0 | 0 |
| Tet1 | tet oncogene 1 | 313.9 | 157.8 | 157.1 | 119.2 | 0.503 | 0.5 | 0.38 | 0 | 0 | 0 |
| Igf1 | Insulin-like growth factor 1 | 383.8 | 306.6 | 183.9 | 203.1 | 0.799 | 0.479 | 0.529 | 0.289 | 0.001 | 0.003 |
| Gng4 | Guanine nucleotide binding protein (G protein), gamma 4 | 360.1 | 218.2 | 159.7 | 182.7 | 0.606 | 0.443 | 0.507 | 0.033 | 0.002 | 0.006 |
| LOC100048058 | Similar to solute carrier family 29 (nucleoside transporters), member 4///solute carrier family 29 (nucleoside transporters), member 4 | 433 | 289.8 | 247 | 199.5 | 0.67 | 0.57 | 0.461 | 0 | 0 | 0 |
| Marcksl1 | MARCKS-like 1 | 3538.6 | 2292.1 | 1849.2 | 1445.6 | 0.648 | 0.523 | 0.409 | 0.012 | 0.001 | 0 |
| Ppp1r14c | Protein phosphatase 1, regulatory (inhibitor) subunit 14c | 349.8 | 263.4 | 225.4 | 168.4 | 0.753 | 0.644 | 0.481 | 0.046 | 0.005 | 0 |
| Crym | Crystallin, mu | 792.8 | 618.1 | 555.5 | 387.2 | 0.78 | 0.701 | 0.488 | 0.811 | 0.498 | 0.057 |

(*continued on next page*)

**Table 1** (*continued*)

| Gene symbol | Gene title | GC (P15) | GC (P20) | GC (P23) | GC (P30) | Change (fold) P20/P15 | P23/P15 | P30/P15 | FDR (Tukey) P15 vs P20 | P15 vs P23 | P15 vs P30 |
|---|---|---|---|---|---|---|---|---|---|---|---|
| 9930013L23Rik | RIKEN cDNA 9930013L23 gene | 424.4 | 257.1 | 243.4 | 200.3 | 0.606 | 0.574 | 0.472 | 0.001 | 0.001 | 0 |
| Dnmt3a | DNA methyltransferase 3A | 1371.1 | 878.7 | 781.3 | 630.2 | 0.641 | 0.57 | 0.46 | 0 | 0 | 0 |
| Tubb2b | Tubulin, beta 2B | 2417.4 | 1555.7 | 1424.9 | 1183.3 | 0.644 | 0.589 | 0.49 | 0.007 | 0.002 | 0 |
| Rras2 | Related RAS viral (r-ras) oncogene homolog 2 | 535.2 | 333.5 | 315.5 | 248.6 | 0.623 | 0.589 | 0.464 | 0.001 | 0 | 0 |
| Lsm11 | U7 snRNP-specific Sm-like protein LSM11 | 282.8 | 190.2 | 170.4 | 126.8 | 0.673 | 0.603 | 0.448 | 0.008 | 0.002 | 0 |
| Lgtn | Ligatin | 227.5 | 146 | 150.6 | 110 | 0.642 | 0.662 | 0.484 | 0 | 0 | 0 |
| Col3a1 | Collagen, type III, alpha 1 | 379.2 | 249.9 | 266.7 | 180.6 | 0.659 | 0.703 | 0.476 | 0 | 0 | 0 |
| Cbln1 | Cerebellin 1 precursor protein | 283.8 | 163.5 | 182.3 | 135.3 | 0.576 | 0.642 | 0.477 | 0.114 | 0.225 | 0.028 |
| Dnmt3a | DNA methyltransferase 3A | 351.6 | 208.4 | 205.1 | 175.1 | 0.593 | 0.583 | 0.498 | 0.009 | 0.007 | 0.001 |
| Dcx | Doublecortin | 319.4 | 215.7 | 179 | 156.4 | 0.675 | 0.56 | 0.49 | 0.03 | 0.004 | 0.001 |
| Rras2 | Related RAS viral (r-ras) oncogene homolog 2 | 368 | 237.4 | 184.7 | 158.6 | 0.645 | 0.502 | 0.431 | 0.001 | 0 | 0 |
| Marcksl1 | MARCKS-like 1 | 2001.1 | 1313.9 | 1020.5 | 780.1 | 0.657 | 0.51 | 0.39 | 0.004 | 0 | 0 |
| Slc16a1 | Solute carrier family 16 (monocarboxylic acid transporters), member 1 | 1894.9 | 1161.5 | 914.8 | 810.1 | 0.613 | 0.483 | 0.428 | 0 | 0 | 0 |
| Apcdd1 | Adenomatosis polyposis coli down-regulated 1 | 636.2 | 478.9 | 347.9 | 311.2 | 0.753 | 0.547 | 0.489 | 0.001 | 0 | 0 |
| Igf1 | Insulin-like growth factor 1 | 390.5 | 317.6 | 217.2 | 189.8 | 0.813 | 0.556 | 0.486 | 0.513 | 0.012 | 0.003 |
| Dynlt1 | Dynein light chain Tctex-type 1///dynein light chain Tctex-type 1, pseudogene 1 /// similar to tctex-1 protein | 1129.9 | 719.6 | 556.4 | 424 | 0.637 | 0.492 | 0.375 | 0.002 | 0 | 0 |
| Npnt | Nephronectin | 416.4 | 290.3 | 228.7 | 201.4 | 0.697 | 0.549 | 0.484 | 0.389 | 0.074 | 0.029 |
| E130309F12Rik | RIKEN cDNA E130309F12 gene | 254.3 | 186.8 | 157.1 | 116.8 | 0.735 | 0.618 | 0.459 | 0.088 | 0.01 | 0.001 |
| Kif21b | Kinesin family member 21B | 475.6 | 305.4 | 261.4 | 209.6 | 0.642 | 0.55 | 0.441 | 0.002 | 0 | 0 |
| Deaf1 | Deformed epidermal autoregulatory factor 1 (Drosophila) | 423.2 | 266.1 | 242.6 | 206.9 | 0.629 | 0.573 | 0.489 | 0 | 0 | 0 |
| Gng4 | Guanine nucleotide binding protein (G protein), gamma 4 | 2271.3 | 1427.4 | 1101.2 | 1053.2 | 0.628 | 0.485 | 0.464 | 0.073 | 0.008 | 0.006 |
| Met | met proto-oncogene | 279.5 | 179.7 | 141.3 | 131.4 | 0.643 | 0.506 | 0.47 | 0.003 | 0 | 0 |
| Dynlt1 | Dynein light chain Tctex-type 1 /// dynein light chain Tctex-type 1, pseudogene 1 /// similar to tctex-1 protein | 2057.6 | 1250.3 | 939 | 904.1 | 0.608 | 0.456 | 0.439 | 0 | 0 | 0 |
| Dnmt3a | DNA methyltransferase 3A | 1437.8 | 887.3 | 704.1 | 552.7 | 0.617 | 0.49 | 0.384 | 0 | 0 | 0 |
| Npnt | Nephronectin | 326.4 | 196 | 168.8 | 142.1 | 0.6 | 0.517 | 0.435 | 0.289 | 0.122 | 0.044 |
| Col1a2 | Collagen, type I, alpha 2 | 206.1 | 131.3 | 95.8 | 66.9 | 0.637 | 0.465 | 0.325 | 0.003 | 0 | 0 |
| Cd24a | CD24a antigen | 219.6 | 140.2 | 94.7 | 73.6 | 0.638 | 0.431 | 0.335 | 0.077 | 0.003 | 0.001 |
| Cd24a | CD24a antigen | 282.3 | 159.8 | 119.6 | 71 | 0.566 | 0.424 | 0.252 | 0.003 | 0 | 0 |
| Aplnr | Apelin receptor | 242 | 92.9 | 88 | 67.5 | 0.384 | 0.364 | 0.279 | 0 | 0 | 0 |

than 147 at 256 gradation image data, which was interpreted as a positive punctate signal.

## 3. Results and discussion

### *3.1. Expression analysis in gustatory and somatosensory cortices at weaning*

To investigate the effects of food intake on child brain development, we performed a microarray analysis of the murine gustatory and somatosensory cerebral cortices throughout the weaning period (Fig. 1). Given free access to a solid food supply, mouse pups began to eat the solid food (OA-2, CLEA Japan) on postnatal day 19. Mouse pups continued to drink mother's milk even after food intake until postnatal week 4. Based on this observation, we determined that postnatal days 19–28 represented the weaning stage in our study. The body weight of the pups gradually increased during weaning with a solid food supply, whereas pups drinking only mother's milk without a solid food supply did not show a comparable weight gain (not shown). This finding suggests that a food supply other than breast milk is necessary for normal infant development at weaning.

Based on this observation of the feeding behavior of murine pups during weaning, we decided to analyze the whole-genome expression profile of the gustatory and somatosensory cortices on postnatal days 15, 20, 23, and 30 (Fig. 1A). A microarray analysis of the whole genes revealed that 31 and 35 genes are down- and upregulated, respectively, during the time from postnatal day 15 to postnatal days 20–30, respectively (Fig. 1B and Table 1). Among 45,037 murine genes on the Affymetrix GeneChip, we selected genes whose expression signal intensity was more than 200 and significantly different from FDR analysis at less than 0.20 and the expression increase of which was less than 0.5-fold or more than 2.0-fold. Of the total genes, 98.3% did not display significant changes in expression during weaning. Changes in expression over time are shown in a heat map analysis for all 66 genes (Fig. 1B). Expression intensity and change over time are variable from gene to gene for both the downregulated (left panels) and upregulated (right panels) genes, respectively. Fold difference analysis indicated the entire pattern of time-course changes of downregulated (Fig. 1C) and upregulated genes (Fig. 1D).

The 31 downregulated genes are mainly involved in organ morphogenesis, tumor formation, and cell growth and differentiation (Table 1A). Among the 31 genes, we identified five cytoskeletal protein genes: MARKS-like 1, tubulin beta 2B, double cortin, dynein light chain Tctex-type 1, and KIF 21B (Table 1A). These genes regulate neural morphology, such as neurite formation and intracellular transport, by modulating the microfilament and microtubule network. We also found four oncogenes: src-like adaptor, tet oncogene 1, r-ras oncogene homolog 2, and met proto-oncogene. These genes regulate cell division and/or cell differentiation.

In contrast, the 35 upregulated genes are mainly involved with the immediate early response to neuronal activation, myelin formation, and glial cell differentiation (Table 1). Among the 35 genes, we identified five immediate early genes: egr-2/Krox-20, Ier-3, Ier-5, arc and homer (Table 1B). Egr-2/Krox-20 is a transcription factor that is activated by neuronal excitation and regulates the transcription of subsets of genes to modulate neuronal functions [24,25]. Those immediate early genes are known to play a pivotal role in neural plasticity by neuronal excitation [26,27], suggesting they are candidate genes that respond to food intake stimulation in the gustatory and somatosensory cortices. Within the upregulated

genes, we also found three glial myelin formation genes – Mog, Mobp, and Mal – which are involved in glial cell differentiation for myelin formation around neuronal axons.

### 3.2. In situ hybridization analysis of the Egr-2/Krox-20 gene at the somatosensory cortex during weaning

During postnatal development, neuronal migration in the cerebral cortex is largely completed by postnatal day 14, followed by a period of neurite elongation, axon myelination, and glial maturation [23]. Based on the microarray analysis, we found five immediate early genes whose expression is activated by neuronal excitation. These are good candidates for food-intake-dependent genes in the gustatory and somatosensory cortices. Immediately after beginning food intake on postnatal day 20, the expression of Egr-2/Krox-20, Ier-3, Ier-5, arc, and homer was upregulated 1.95-, 1.40-, 1.63-, 1.53-, and 1.84-fold, respectively, when compared to their expression before weaning on postnatal day 15 (Table 1B). Because Egr-2/Krox-20 is the most upregulated among the five candidates, we decided to investigate Egr-2/Krox-20 [24,25] in further detail using an *in situ* hybridization technique (Fig. 2).

First, we analyzed the localization of Egr-2/Krox-20 mRNA in the somatosensory cortex on postnatal day 15 (Fig. 2A) and day 22 (Fig. 2B). Before weaning, Egr-2/Krox-20 mRNA is localized in the nucleus at layer 5/6 of the somatosensory cortex (Fig. 2A). Egr-2/Krox-20 mRNA appears to be expressed in pyramidal neurons based on the location of the cell body in layer 5/6, the density of cell number in layer 5/6, and the size of the nucleus (Fig. 2A). Three days after starting solid foods, however, Egr-2/Krox-20 mRNA is not only located in the nucleus but also throughout the cytosol (Fig. 2B). Generally, messenger RNA is synthesized, edited in the nucleus, transported from nucleus to cytosol, and translated on ribosomes. Together with the microarray data, we concluded that Egr-2/Krox-20 mRNA is not only upregulated but also transported from the nucleus to the cytosol during weaning. Statistical analysis of the *in situ* hybridization data clearly indicated that the number of cytosolic mRNA punctate is significantly increased by approximately 3-fold (Fig. 2C).

### 3.3. In situ hybridization analysis of Egr-2/Krox-20 genes in the somatosensory cortex with or without solid food

Egr-2/Krox-20 is known to be induced by various extracellular stimuli, such as growth factors and neuronal excitation, and it plays a role as a transcriptional co-activator [23,24]. Thus, it is possible that chemical, textural, and nutritional stimulation by food intake may evoke its expression. To address this question, we performed an *in situ* hybridization analysis using samples taken on postnatal day 22 from weaning mice and from mice that were kept exclusively on a diet of mother's milk (Fig. 3). We analyzed the localization of Egr-2/Krox-20 mRNA in the somatosensory cortex on postnatal day 22 without (Fig. 3A) or with (Fig. 3B) solid food. In the absence of a solid food supply, Egr-2/Krox-20 mRNA is localized in the nucleus of giant pyramidal neurons in layer 5 of the somatosensory cortex on postnatal day 22 (Fig. 3A). In the presence of a solid food supply, however, Egr-2/Krox-20 mRNA is located throughout the cell body and dendrites as well as in the nucleus (Fig. 3B). We concluded that Egr-2/Krox-20 mRNA is not only upregulated but also transported from nucleus to cytosol following solid food supply. Statistical analysis of the *in situ* hybridization data clearly indicated that the number of cytosolic mRNA punctate significantly increased by threefold (Fig. 3C).

In this study, we report the time course of the whole-gene expression profile in the mouse gustatory and somatosensory cortex during the weaning period. Among 14,000 genes tested, 31 and 35 genes are down- and upregulated, respectively, during weaning. Among these genes, an immediate early response gene, Egr-2/Krox-20, is transported from the nucleus to the cytosol in layer 5 of the somatosensory cortex by solid food intake. The Egr-2/Krox-20 gene is upregulated by neurotropic factors or electric nerve stimulation and plays a central role in neural differentiation as a transcription factor [24,25].

In conclusion, we showed in this study that weaning in mice induces, among other effects, the expression of Egr-2/Krox-20,

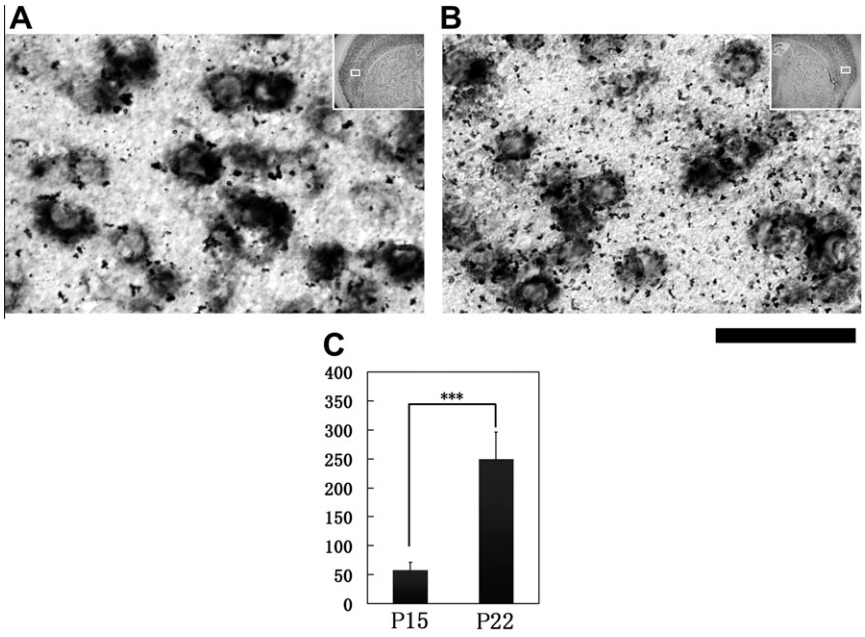


**Fig. 2.** *In situ* hybridization of Egr-2/Krox-20 (A, B) at postnatal days 15 (A) and 22 (B) in the somatosensory cortex. The black bar in the lower right corner indicates 50 μm. Inset: An *in situ* hybridization image of the whole hemisphere under low-magnification microscopic observation on postnatal day 15 (A) and day 22 (B). White boxes in the insets indicate the area observed at high magnification. (C) The mean number of extra-nuclear punctate of Egr-2/Krox-20 per 15,000 $\mu m^2$. P15: postnatal day 15; P22: postnatal day 22. Error bars indicate the standard deviation. Triple asterisks indicate significant difference ($n = 9$, $P < 0.005$).

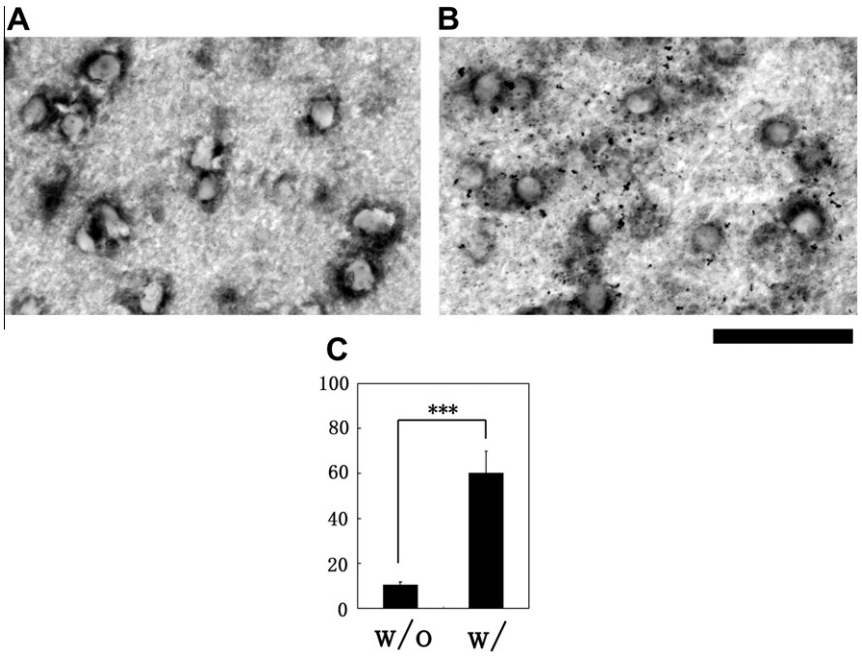


**Fig. 3.** *In situ* hybridization of Egr-2/Krox-20 with (A) or without (B) solid food intake stimulation in the somatosensory cortex. The black bar in the lower-right corner indicates 50 μm. (C) Mean number of extra-nuclear punctate of Egr-2/Krox-20 per 15,000 μm$^2$. Error bars indicate the standard deviation. Triple asterisks indicate significant difference ($n = 9$, $P < 0.005$).

encoding a transcription factor at the somatosensory cortex. Based on our data, we propose a hypothesis that food intake signals induce an Egr-2/Krox-20 transcription factor, which may play a role in cognition, learning, and memory of the natural food environment during weaning. In the future, it will be important to determine whether the taste/texture signals or the nutritional factors of solid food evoke gene expression at the weaning stage.

Recently, we also reported that solid food intake induced the accumulation of SNAP25, a component of the SNARE complex, in the gustatory and somatosensory cortices during weaning [20]. Taken together, these results suggest that changes in food intake may play an important role in brain development and function in weaning children.

## Acknowledgments

We would like to express our special thanks to Dr. Jeffrey D. Millbrandt (Washington University, MO) and Dr. Jay Baraban (Johns Hopkins University Medical School, MD) for the generous gift of the Egr-2/Krox-20 cDNA clone. We thank Dr. Azusa Kurokawa and Mr. Shunsuke Itoh (The University of Tokyo, Japan) for technical advice on the *in situ* hybridization and microarray data analysis. This work was partly supported by a grant from Nestec Co. (to K.A.); the Funding Program for Next Generation World-Leading Researchers from the Japan Society for the Promotion of Science (LS037 to T.M.); a grant from the Iijima Memorial Foundation for the Promotion of Food Science and Technology (to H.A.); and a grant-in-aid for scientific research from the Ministry of Education, Culture, Sports, Science and Technology of Japan (21780121 to M.O. and 23248058 to K.A.).

## References

[1] L.L. Birch, Effects of experience on the modification of food acceptance patterns, Annals NY Acad. Sci. 561 (1989) 209–216.
[2] D.A. Yarmolinsky, C.S. Zuker, N.J.P. Ryba, Common sense about taste: from mammals to insects, Cell 139 (2009) 234–244.
[3] R. Margolskee, Molecular mechanisms of bitter and sweet taste transduction, J. Biol. Chem. 277 (2002) 1–4.
[4] A. Brockhoff, M. Behrens, M.Y. Niv, W. Meyerhof, Structural requirements of bitter taste receptor activation, Proc. Natl. Acad. Sci. USA 107 (2010) 1110–1115.
[5] S.D. Roper, N. Chaudhari, Processing umami and other taste in mammalian taste buds, Annals NY Acad. Sci. 1170 (2009) 60–65.
[6] K. Abe, Studies on taste: molecular biology and food science, Biosci. Biotechnol. Biochem. 72 (2008) 1647–1656.
[7] M. Majdan, C. Shatz, Efects of visual experience on activity-dependent gene regulation in cortex, Nat. Neurosci. 9 (2006) 650–659.
[8] J.A. Mennella, A.K. Ventura, Early nutrition: impact on short- and long-term health, Nestlé Nutr. Workshop Ser. Pediatr. Program. 68 (2011) 153–163.
[9] S.D. Roper, Cell communication in taste buds, Cell. Mol. Life Sci. 63 (2006) 1494–1500.
[10] M. Ohmoto, I. Matsumoto, A. Yasuoka, Y. Yoshihara, K. Abe, Genetic tracing of the gustatory and trigeminal neural pathways originating from T1R3-expressing taste receptor cells and solitary chemoreceptor cells, Mol. Cell. Neurosci. 38 (2008) 505–517.
[11] M. Ohmoto, N. Maeda, K. Abe, Y. Yoshihara, I. Matsumoto, Genetic tracing of the neural pathway for bitter taste in t2r5-WGA transgenic mice, Biochem. Biophys. Res. Commun. 400 (2010) 734–738.
[12] T. Yamamoto, Taste response of cortical neurons, Prog. Neurobiol. 23 (1984) 273–315.
[13] E. Kosar, H.J. Grill, R. Norgren, Gustatory cortex in the rat. I. Physiological properties and cytoarchitecture, Brain Res. 379 (1986) 329–341.
[14] D.H. Zald, M.C. Hagen, J.V. Pardo, Neural correlates of tasting concentrated quinine and sugar solutions, J. Neurophysiol. 87 (2001) 1068–1075.
[15] M.A. Schoenfeld, G. Neuer, C. Tempelmann, K. Schussler, T. Noesselt, J.-M. Hopf, H.-J. Heinze, Functional magnetic resonance tomography correlates of taste perception in the human primary taste cortex, Neuroscience 127 (2004) 347–353.
[16] R. Accolla, B. Bathellier, C.C.H. Petersen, A. Carleton, Differential spatial representation of taste modalities in the rat gustatory cortex, J. Neurosci. 27 (2007) 1396–1404.
[17] K. Ohla, U. Toepel, J. le Coutre, J. Hudry, Electrical neuroimaging reveals intensity-dependent activation of human cortical gustatory and somatosensory areas by electric taste, Biol. Psychol. 85 (2010) 446–455.
[18] M. Kobayashi, S. Fujita, H. Takei, L. Song, S. Chen, I. Suzuki, A. Yoshida, K. Iwata, N. Koshikawa, Functional mapping of gustatory neurons in the insular cortex revealed by pERK-immunohistochemistry and *in vivo* optical imaging, Synapse 64 (2010) 323–344.
[19] X. Chen, M. Gabitto, Y. Peng, N.J. Ryba, C.S. Zuker, A gustotopic map of taste qualities in the mammalian brain, Science 333 (2011) 1262–1266.
[20] S. Kawakami, M. Ohmoto, S. Ohmoto, R. Yuasa, H. Inagaki, E. Nishimura, T. Ito, T. Misaka, Accumulation of SNAP25 in mouse gustatory and somatosensory corteces in response to food and chemical stimulation, Neuroscience 218 (2012) 326–334.
[21] M. Mayford, S.A. Siegelbaum, E.R. Kandel, Synapses and memory storage, Cold Spring Harb. Perspect. Biol. 4 (2012) a005751.

[22] N. Maeda, M. Onimura, M. Ohmoto, T. Inui, T. Yamamoto, I. Ichiro, K. Abe, Spatial differences in molecular characteristics of the pontine parabrachial nucleus, Brain Res. 1296 (2009) 24–34.
[23] A.W. Lyckman, S. Horng, C.A. Leamey, D. Tropea, A. Watakabe, A.V. Wart, C. McCurry, T. Yamamori, M. Sur, Gene expression patterns in visual cortex during the critical period: synaptic stabilization and reversal by visual deprivation, Proc. Natl. Acad. Sci. USA 105 (2008) 9409–9414.
[24] R.V. Bhat, P.F. Worley, A.J. Cole, J.M. Baraban, Activation of the zinc finger encoding gene krox-20 in adult rat brain: comparison with zif268, Brain Res. Mol. Brain Res. 13 (1992) 263–266.
[25] J. Svaren, B.R. Sevetson, E.D. Apel, D.B. Zimonjic, N.C. Popescu, J. Milibandt, NAB2, a corepressor of NGFI-A (Egr-1) and Krox20, is induced by proliferative and differentiative stimuli, Mol. Cell. Biol. 16 (1996) 3545–3553.
[26] H. Okuno, Regulation and function of immediate-early genes in the brain: beyond neuronal activity markers, Neurosci. Res. 69 (2011) 175–186.
[27] C.R. Bramham, P.F. Worley, M.J. Moore, J.F. Guzowski, The immediate early gene *Arc/Arg3.1*: regulation, mechanisms, and function, J. Neurosci. 28 (2008) 11760–11767.